PERGAMON

Available online at www.sciencedirect.com

SCIENCE DIRECT®

Polyhedron 22 (2003) 1481–1487

POLYHEDRON

www.elsevier.com/locate/poly

Synthesis, X-ray crystal structure, and solution properties of nickel(II) complexes of new 16-membered mixed-donor macrocyclic Schiff base ligand incorporating a pendant alcohol function

Ali Akbar Khandar [a,*], Seyed Abolfazl Hosseini-Yazdi [a,b]

[a] *Department of Inorganic Chemistry, Faculty of Chemistry, Tabriz University, Tabriz 51664, Iran*
[b] *Iranian R&D Center for Chemical Industries, PO Box 14155-4364, Tehran, Iran*

Received 9 December 2002; accepted 5 March 2003

Abstract

The synthesis of N_2O_3 macrocyclic ligand 8,9,18,19-tetrahydro-7H,17H-dibenzo[f,o][1,5,9,13] dioxadiazacyclohexadecin-18-ol (L = **2**) and preparation of complexes $NiLX_2$ (X = Cl, Br, I, ClO_4) and NiLXY (X = Cl, Br, I and Y = ClO_4) are reported. $NiLX_2$ complexes were prepared by facile template reactions of appropriate dialdehyde 2-[3-(2-formylphenoxy)-2-hydroxypropoxy]bezaldehyde (**1**) and 1,3-diaminopropane in the presence of Ni(II) salts. Reactions of $NiL(ClO_4)_2$ (**2d**) with lithium halides resulted in NiLXY complexes. From spectroscopic measurements and conductivity studies of the complexes it is followed that the six-coordinate species $NiLX^+$ are formed in solution except **2d**. In all complexes the ligand behaves as a pentadentate ligand. Complexes **2b**·CH_3CN and **2b**·1.75CH_3CN (**2b** = $NiLBr_2$) contain nickel in a distorted octahedral environment of N_2O_3Br donors.

Keywords: Macrocycle; Schiff base; Template; Nickel(II) complexes; Mixed-donor macrocycles; Azacrown ethers

1. Introduction

Crown ethers possess attractive cation binding properties towards non-transition metals such as the alkali and alkaline-earth metal ions [1]. Crown ethers in which some of the oxygen atoms are replaced by nitrogen atoms, named azacrown ethers, are known to show great affinity for softer metal ions than alkali and alkaline-earth ions. The interaction of metal ions with oxygen–nitrogen donor macrocycles has been the subject of a range of studies. A number of these investigations have been involved synthetic [2–5], kinetic [6,7], thermodynamic [8–10], and structural aspects [11–13] of complex formation with a range of metal ions. The capacity of nickel to bind both hard and soft donor ligands allows its coordination chemistry to encompass a variety of geometries, coordination numbers, and oxidation states with its reactivity in biological to organometallic chemistry [14–16]. The hydroxyl group at the C-backbone in macrocycle has been chosen because it is easily transformed to amines or other substituents with linking potential for attachment to other substrates to produce, for example, immobilised systems for metal-ion scavenging [17,18]. Herein we report the synthesis and characterization of Ni(II) complexes which contain several counterions. To gain insight into the solid-state structures of the present complexes, X-ray diffraction studies of some complexes have been undertaken.

2. Experimental

2.1. Materials

Solvents were dried and purified before being used according to published procedures [19,20]. $NiCl_2$, $NiBr_2$, NiI_2, $Ni(ClO_4)_2·6H_2O$ [21] and 1,3-dibromo-2-propanol [22] were prepared according to literature methods. Other reagents were obtained from Merck or Fluka

---

[*] Corresponding author. Tel.: +98-41-1334-6494; fax: +98-41-1334-0191.
E-mail address: khandar@tabrizu.ac.ir (A.A. Khandar).

doi:10.1016/S0277-5387(03)00124-4

and used as received. Caution: although we have not experienced difficulties with the perchlorate salts, these should be regarded as potentially explosive and handled with care.

2.2. Physical measurements

^1H and ^{13}C NMR spectra were taken on a Bruker Avance 400 spectrometer in $CDCl_3$ at 400.13 and 100.61 MHz, respectively. The chemical shifts (in ppm) were referenced with respect to the residual solvent signal or TMS. FT-IR spectra were obtained on a BOMEM MB 100 instrument using KBr pellets. Mass spectra were recorded on a Finnigan mass spectrometer. Electronic spectra were measured on Shimatzu UV-2100 Spectrophotometer and quartz cells of light path length 1.00 cm. Elemental analyses were performed with an elemental analyzer CHN-O-RAPID, Heraeus. All melting points were taken using an electrothermal IA 9100 apparatus in open capillary tubes and are uncorrected. Conductance measurements were performed using a Hanna HI 8820 Conductance meter. The conductivity cell was calibrated with aqueous KCl. Freshly distilled CH_3NO_2 (distilled from CaH_2 under N_2) used in the conductivity measurements and spectrophotometric studies was found to have conductivity in the range of $(2–5) \times 10^{-6}$ Ω^{-1} cm^{-1}.

2.3. Syntheses

2.3.1. 2-[3-(2-Formylphenoxy)-2-hyroxypropoxy]benzaldehyde (**1**)

2-[3-(2-Formylphenoxy)-2-hyroxypropoxy]benzaldehyde was prepared by the method of Lindoy and Armstrong [23] with minor modification. Sodium hydroxide (8.0 g, 0.2 mol) in water (400 ml) was added to salicylaldehyde (24.45 g, 0.2 mol) in ethanol (20 ml). The mixture was warmed and 1,3-dibromo-2-propanol (21.79 g, 0.1 mol) was added. Sufficient ethanol (270 ml) to produce a homogeneous solution was then added. The solution was refluxed under nitrogen for 70 h, then cooled and let stand at 0 °C. The cream-colored solid product was washed with water. The solid product was recrystallized in 2:1 (ethanol–water). The resulting crystals were collected by filtration and dried in a vacuum desiccator over P_4O_{10}. Yield 11.45 g (38%), m.p. 114 °C. *Anal.* Calc. (Found) for $C_{17}H_{16}O_5$: C, 67.99 (68.07); H, 5.37 (5.28)%. Mass spectral parent ion; *m/z* 300.1. ^1H NMR ($CDCl_3$) δ 10.44 (s, 2H, 2ArCHO); 7.82 (d, 2H, 2ArH); 7.57 (t, 2H, 2ArH); 7.03–7.18 (m, 4H, 4ArH); 4.50 (quintet, 1H, CH); 4.33 (d, 4H, CH_2); 3.29 (s (broad), 1H, OH washed out by D_2O) ppm. ^{13}C NMR ($CDCl_3$) δ 190.423 (CHO); 160.871, 136.632, 130.148, 125.303, 121.781, 113.290 (Ar); 69.815 (OCH_2); 68.733 (CHOH) ppm. Selected FT-IR data, ν (cm^{-1}): 3469s (OH), 3107w, 2943m, 2876m, 2840w, 2758w, 1679s (C=O), 1599s, 1486s, 1248s, 1164m, 1032s, 844m, 759s, 661m.

2.3.2. $NiLCl_2$ (**2a**)

A 1-butanol solution (50 ml) of 1,3-diaminopropane (0.3716 g, 5 mmol) was added slowly with stirring to a 150 ml hot 1-butanol solution of **1** (1.5015 g, 5 mmol) and $NiCl_2$ (0.6481 g, 5 mmol). The solution was stirred and refluxed for 2 h, its color shifted to green. The volume was reduced to 50 ml by using a rotary evaporator. The resultant green solid product was collected by filtration and recrystallized from butanol. The resulting green crystals were filterated and dried in a vacuum desiccator over P_4O_{10}. Yield 1.84 g (77%). It decomposes above 231 °C. *Anal.* Calc. (Found) for $C_{20}H_{22}Cl_2N_2NiO_3.0.5H_2O$: C, 50.36 (50.24); H, 4.86 (5.05); N, 5.87 (6.00)%. Selected FT-IR data, ν (cm^{-1}): 3418m, 3258m, 3051w, 2928m, 1637s (C=N), 1604s, 1494s, 1443m, 1213s, 1073m, 990s, 811m, 772s, 460m.

2.3.3. $NiLBr_2$ (**2b**)

In a manner similar to the above-mentioned a 1-butanol solution (50 ml) of 1,3-diaminopropane (0.2973 g, 4 mmol) was added with stirring to a 125 ml hot 1-butanol solution of **1** (1.2012 g, 4 mmol) and $NiBr_2$ (0.874 g, 4 mmol). The solution was stirred and refluxed for 1 h, its color shifted to green. The volume was reduced to 50 ml by using a rotary evaporator. The resultant green solid was collected by filtration and recrystallized from butanol. The resulting needle green crystals were collected by filtration and dried in a vacuum desiccator over P_4O_{10}. Yield 1.58 g (70%). It decomposes above 235 °C. *Anal.* Calc. (Found) for $C_{20}H_{22}Br_2N_2NiO_3.0.5H_2O$: C, 42.45 (42.22); H, 4.10 (4.15); N, 4.95 (5.00)%. Selected FT-IR data, ν (cm^{-1}): 3433m, 3310m, 3042w, 2928m, 1636s (C=N), 1603s, 1492m, 1442m, 1211s, 1120m, 989s, 810m, 773s, 460m.

2.3.4. $NiLI_2$ (**2c**)

In the same way a 1-butanol solution (50 ml) of 1,3-diaminopropane (0.2973 g, 4 mmol) was added with stirring to a 125 ml hot 1-butanol solution of **1** (1.2012 g, 4 mmol) and NiI_2 (1.2513 g, 4 mmol). The solution was stirred and refluxed for 1 h. The resultant olive-green solid was filtered, and washed sparingly with 1-butanol and dried in vacuum desiccator over P_4O_{10}. Yield 1.6 g (61%). It decomposes above 245 °C. *Anal.* Calc. (Found) for $C_{20}H_{22}I_2N_2NiO_3$: C, 36.91 (36.64); H, 3.41 (3.46); N, 4.30 (4.23)%. Selected FT-IR data, ν (cm^{-1}): 3428m, 3207m, 3052w, 2933w, 1635s (C=N), 1604s, 1577m, 1493m, 1281m, 1211s, 1120m, 1072m, 990s, 899m, 811m, 772s, 462m.

2.3.5. $NiL(ClO_4)_2$ (**2d**)

A 1-butanol solution (50 ml) of 1,3-diaminopropane (0.2224 g, 3 mmol) was added slowly with stirring to a

80 ml hot 1-butanol solution of **1** (0.9009 g, 3 mmol) and $Ni(ClO_4)_2.6H_2O$ (1.0971 g, 3 mmol). The solution was stirred and refluxed for 2 h, then filtered. The volume of filtrate was reduced to 40 ml by using a rotary evaporator. The resultant solid product was collected by filteration and recrystallized from 1-butanol. The resulting needle blue–green crystals were collected and dried in vacuum desiccator over P_4O_{10}. Yield 1.11 g (62%). It decomposes above 300 °C. *Anal.* Calc. (Found) for $C_{20}H_{22}Cl_2N_2NiO_{11}$: C, 40.31 (39.72); H, 3.72 (3.67); N, 4.70 (4.72)%. Selected FT-IR data, ν (cm^{-1}): 3423m, 3067w, 2928w, 2856w, 1637s (C=N), 1604s, 1494m, 1446m, 1210s, 1109s, 1083s, 986m, 810m, 769s, 626s, 460m.

2.3.6. NiL(Cl)ClO$_4$ (**2ad**)

A methanol solution (20 ml) of $LiCl.H_2O$ (0.0604 g, 1 mmol) was added slowly with stirring to a boiling solution of $NiL(ClO_4)_2$ (0.5960 g, 1 mmol) in 1-butanol (30 ml). The solid separated product was collected and washed with 1-butanol. The product was recrystallized from acetonitrile. The resulting green crystals were collected by filtration and dried in a vacuum desiccator over P_4O_{10}. Yield 0.5008 g (94%). It decomposes above 310 °C. *Anal.* Calc. (Found) for $C_{20}H_{22}Cl_2N_2NiO_7$: C, 45.15 (45.21); H, 4.17 (4.20); N, 5.27 (5.31)%. Selected FT-IR data, ν (cm^{-1}): 3443m, 3012s, 1641s (C=N), 1605s, 1577s, 1494s, 1442s, 1311m, 1284s, 1211s, 1094s, 1015s, 986s, 810m, 776s, 623s, 462m.

2.3.7. NiL(Br)ClO$_4$ (**2bd**)

Similarly LiBr (0.0869 g, 1 mmol) yielded the product as green crystals. Yield 0.5363 g (93%). It decomposes above 290 °C. *Anal.* Calc. (Found) for $C_{20}H_{22}BrClN_2NiO_7$: C, 41.67 (40.34); H, 3.85 (3.90); N, 4.86 (5.20)%. Selected FT-IR data, ν (cm^{-1}): 3422m, 3178m, 2927w, 1635s (C=N), 1604s, 1578m, 1494m, 1443m, 1261s, 1094s, 990s, 811m, 771s, 623s, 510w.

2.3.8. NiL(I)ClO$_4$ (**2cd**)

Similarly LiI (01339 g, 1 mmol) yielded the product as olive green crystals. Yield 0.6312 g (95%). It decomposes above 270 °C. *Anal.* Calc. (Found) for $C_{20}H_{22}IClN_2NiO_7.CH_3CN$: C, 39.76 (39.90); H, 3.79 (3.90); N, 6.32 (6.11)%. Selected FT-IR data, ν (cm^{-1}): 3428m, 3191m, 2928w, 2856w, 1635s (C=N), 1605s, 1493s, 1210s, 1092s, 989s, 811m, 771s, 623s, 460m.

2.3.9. Preparation of (8,9,18,19–tetrahydro-7H,17H-dibenzo [f,o][1,5,9,13] dioxadiazacyclohexadecin-18-ol) (L = 2)

The literature procedure was used from Ref. [23]. 1,3-Diaminopropane (6 mmol) in absolute methanol (10 ml) was added to a stirred solution of $NiLX_2$ (X = Cl, Br or I) (2 mmol) in absolute methanol (15 ml). The suspension was stirred at room temperature for 30 min. After filtration the macrocycle was precipitated by the addition of water. The cream-colored solid product was recrystallized from petroleum ether–dichloromethane and dried in a vacuum desiccator over P_4O_{10}. Yield 0.32 g (47% for $NiLCl_2$), 0.28 g (41% for $NiLBr_2$), 0.25 g (37% for $NiLI_2$), m.p. 122–123 °C. *Anal.* Calc. (Found) for $C_{20}H_{22}N_2O_3$: C, 70.78 (70.33); H, 6.55 (6.43); N, 8.28 (8.28)%. Mass spectral parent ion; m/z 338.1. ^1H NMR ($CDCl_3$) δ 8.69 (s, 2H, 2ArCHN); 7.98 (d, 2H, 2ArH); 7.44 (t, 2H, 2ArH); 7.09 (t, 2H, 2ArH); 7.08 (d, 2H, 2ArH); 4.36 (m, 5H, $CH_2CH(OH)CH_2$); 3.63 (t, 4H, NCH_2); 2.99 (quintet, 2H, $CH_2CH_2CH_2$) ppm. ^{13}C NMR ($CDCl_3$) δ 158.739 (CH=N); 158.657, 132.365, 128.097, 126.380, 122.685, 114.785 (Ar); 72.488 ($CH_2CH(OH)CH_2$); 68.698 ($CH_2CH(OH)CH_2$); 57.558 ($CH_2CH_2CH_2$); 29.186 ($CH_2CH_2CH_2$) ppm. Selected FT-IR data, ν (cm^{-1}): 3209m (OH), 3072w, 2930m, 2845m, 1636s (C=N), 1600s, 1579m, 1485s, 1376s, 1245s, 1160m, 1110s, 963m, 898m, 755s, 636m, 468m.

2.4. X-ray crystallography

Single crystals of **2b**·CH_3CN and **2b**·$1.75CH_3CN$ were obtained from acetonitrile solution and separated by hand. The minor (trace) product, **2b**·$1.75CH_3CN$, was blue. **2b**·CH_3CN,the major product, was green. Single crystal X-ray diffraction data for **2b**·CH_3CN and **2b**·$1.75CH_3CN$ were collected with use of the program SMART [24] on a Bruker Smart 1000 CCD diffractometer. Monochromatized Mo Kα radiation was employed. Cell refinement and data reduction were carried out with the use of the program SAINT-PLUS [25]. An absorption correction was applied using SADABS [26]. The structures were solved using direct methods and refined by full-matrix least-squares procedures using SHELXTL [27]. Scattering factors were taken from International Tables for Crystallography [28]. Details of the X-ray experiments and crystal data are summarized in Table 1.

3. Results and discussion

3.1. Syntheses

Dialdehydes have been used previously as precursors for macrocyclic ligand syntheses since they can often be induced to undergo Schiff base cyclization reactions when allowed to react with diamines. Dialdehyde **1** was prepared by Williamson condensation between salicylaldehyde and 1,3-dibromo-2-propanol as outlined in Scheme 1. The IR and NMR data are in accord with the proposed structure. The infrared spectrum of this dialdehyde shows a carbonyl mode at 1679 cm^{-1} and in ^1H NMR spectrum resonances attributable to aldehydic functions appear as a singlet at 10.44 ppm. The

Table 1
Crystal data and structures refinement parameters for **2b**·CH_3CN and **2b**·$1.75CH_3CN$

	2b·CH_3CN	**2b**·$1.75CH_3CN$
Empirical formula	$C_{22}H_{25}Br_3N_3NiO_3$	$C_{23.5}H_{27.5}Br_2N_{3.75}NiO_3$
Formula weight	597.98	628.88
Temperature (K)	110(2)	110(2)
Wavelength (Å)	0.71073	0.71073
Crystal system	orthorhombic	tetragonal
Space group	$P2_12_12_1$	$P42_1c$
Unit cell dimensions		
a (Å)	8.059(2)	21.077(5)
b (Å)	12.372(3)	21.077(5)
c (Å)	23.578(6)	11.492(4)
α (°)	90	90
β (°)	90	90
γ (°)	90	90
V (Å^3)	2351.0(11)	5105(3)
Z	4	8
D_{calc} (Mg m^{-3})	1.689	1.636
Absorption coefficient (mm^{-1})	4.253	3.922
F(000)	1200	2550
Crystal size (mm)	0.2 × 0.1 × 0.08	0.6 × 0.3 × 0.2
θ Range for data collection (°)	1.86–30.03	1.93–30.15
Limiting indices h,k,l	$-11 \leq h \leq 11$, $-17 \leq k \leq 17$, $-33 \leq l \leq 33$	$-28 \leq h \leq 29$, $-17 \leq k \leq 29$, $-16 \leq l \leq 15$
Reflections collected/unique	27891/6863 [$R_{int} = 0.0726$]	42152/7483 [$R_{int} = 0.1166$]
Transmission (max/min)	0.56/0.26	0.43/0.18
Refinement method	full-matrix least-squares on F^2	full-matrix least-squares on F^2
Data/restraints/parameters	6863/0/281	7483/0/305
Goodness-of-fit on F^2	0.863	0.785
Final R indices [$I > 2\sigma(I)$] [a]	$R_1 = 0.0404$, $wR_2 = 0.0869$	$R_1 = 0.0427$, $wR_2 = 0.0772$
R indices (all data) [a]	$R_1 = 0.0752$, $wR_2 = 0.0943$	$R_1 = 0.1076$, $wR_2 = 0.0870$
Largest difference peak and hole (e Å^{-3})	1.108 and −0.509	1.154 and −0.584

[a] $R_1 = \Sigma||F_o|-|F_c||/\Sigma|F_o|$; $wR_2 = \{\Sigma[w(F_o^2-F_c^2)^2]/\Sigma[w(F_o^2)^2]\}^{1/2}$.

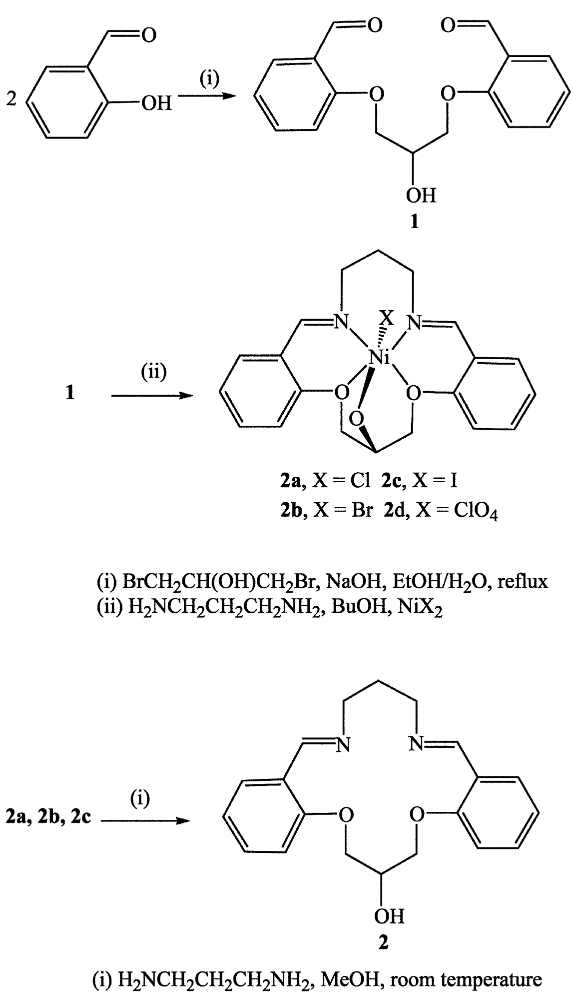

(i) $BrCH_2CH(OH)CH_2Br$, NaOH, EtOH/H_2O, reflux
(ii) $H_2NCH_2CH_2CH_2NH_2$, BuOH, NiX_2

(i) $H_2NCH_2CH_2CH_2NH_2$, MeOH, room temperature

Scheme 1.

condensation of the dialdehyde **1** in the presence of Ni(II), using the conditions described in Section 2, results in isolation of the corresponding complexes of the diimine ligand **2** (see Scheme 1). Conversion of the aldehyde groups into Schiff base derivatives is indicated by the absence of amine and carbonyl absorption (1679 cm^{-1}) bands and appearance of strong bands between 1635–1641 cm^{-1} assignable to the $\nu(C{=}N)_{imine}$ groups [23]. The diperchlorate complex **2d** shows a split perchlorate band at ~1100 cm^{-1}. This may reflects different environments in this complex arising from crystal packing or hydrogen bonding effects; however, the splitting could reflects a lowering of the symmetry of the perchlorate group owing to coordination to nickel ion. In contrast, the infrared spectra of $NiLXClO_4$ complexes contain a non-splitting absorption band at ~1100 cm^{-1} which is typical of non-coordinated perchlorate [29].

Macrocycle **2** was prepared as outlined in Scheme 1. Addition of 3 molar equiv. of 1,3-diaminopropane to a solution of $NiLX_2$ (X = Cl, Br or I) in dry methanol leads to Ni(1,3-diaminopropane)$_3X_2$, and the macrocycle **2**. The macrocycle was isolated from the filtrate by addition of water. IR, NMR, Mass spectral data (see Section 2) and elemental analyses support cyclic Schiff base macrocycle. In ^{1}HNMR spectrum, resonances attributed to aldehydic functions at 10.44 ppm are absent and imine resonances appear as a singlet at 8.69 ppm.

3.2. Solution studies

Some physical and spectrophotometric properties of these complexes are listed in Table 2. The conductance value of $NiL(ClO_4)_2$ complex lies in the range observed for 2:1 electrolytes (150–180 cm^2 Ω^{-1} mol^{-1}) [30] and thus it is a five-coordinate species NiL^{2+} in nitromethane solution. The conductance data for $NiL(X)ClO_4$ complexes revealed that these complexes behave as 1:1 electrolytes (75–95 $cm^2\ \Omega^{-1}\ mol^{-1}$), [30] indicating the presence of six-coordinate species $NiLX^+$ in solution. $NiLX_2$ complexes except **2d** yielded conductance values that fell below of the expected conductance values for 1:1 electrolytes. Hence, under the conditions of measurments, for these complexes significant complex cation–anion association and intermolecular interactions are present in each case, probably because of hydrogen bonding between the adjacent molecules. The increasing of conductance values from Cl^- to I^- in $NiLX_2$ complexes are in agreement with decreasing of strength of hydrogen bonds from Cl^- to I^- (see Section 3.3).

The colors and spectral properties of the complexes confirm the coordination numbers and geometries suggested from the conductivity data. All complexes dissolve in CH_3NO_2 to give green solutions except **2d**. These complexes exhibit three absorption bands, one in the range of 622–635 nm, the other one as shoulders in the range 373–381 nm and a weaker band near 800 nm. In **2c** and **2cd** the shoulders are not observed. If we assume six-coordinate, pseudooctahedral structure for these complexes, the two bands in the range of 622–635 and 373–381 nm can be assigned to the spin-allowed d–d transitions ν_2 ($^3A_{2g} \rightarrow {}^3T_{1g}$) and ν_3 ($^3A_{2g} \rightarrow {}^3T_{1g}(P)$), respectively [31]. The weak band near 800 nm can be assigned to the spin-forbidden transition $^3A_{2g} \rightarrow {}^1E_g$. The color and electronic spectrum patterns of **2a** to **2c** series are similar to their corresponding patterns of **2ad** to **2cd** series. Blue–green crystals of **2d** in CH_3NO_2 solvent give a blue solution. The colors of **2d** in solid state and nitromethane solution are different. The electronic spectrum of **2d** in solution is solvent dependent. In acetonitrile and methanol the main absorption band in nitromethane is shifted from 567 to 569 and 587 nm, respectively. The bands at 381 and 567 nm of **2d** in CH_3NO_2 are shifted to 459 and 782 nm in DMSO. It may be suggested that in DMSO the $NiL(solv)^{2+}$ species is formed. It is inferred from the spectroscopic and conductivity data that all complexes except **2d** form the six-coordinate species $NiLX^+$, but **2d** forms five-coordinate species NiL^{2+} in nitromethane (have low donor capacity) and $NiL(solv)^{2+}$ species in solvents with high donor capacity.

Table 2
Physical/spectroscopic data for complexes

No.	Color	Λ_m [a]	UV–Vis, λ (ε, $M^{-1}\ cm^{-1}$)
	Solid/CH_3NO_2		Nitromethane
2a	green/green	27	373(sh), 627(15), 797(3)
2b	green/green	45	374(sh), 626(30), 812(2)
2c	olive green/olive green	69	622(31), 820(3)
2d	blue green/blue	179	381(sh), 567(15), 839(4)
2ad	green/green	87	376(sh), 631(27), 804(2)
2bd	green/green	94	623(28), 798(2)
2cd	olive green/olive green	95	375(sh), 631(18), 800(3)

[a] Molar conductance ($cm^2\ \Omega^{-1}\ mol^{-1}$) for ca. 10^{-3} M solutions of the compounds in nitromethane at 25 °C.

3.3. X-ray structures

Selected bond lengths and angles of complexes are summarized in Table 3 and ORTEP views are shown in Fig. 1. Complex **2b**·CH_3CN contains nickel in a distorted octahedral coordination environment. The six-coordinate Ni(II) is defined by the two etheric oxygen atoms O(1) and O(2), the two imino nitrogen atoms N(1) and N(2) and by the protonated alcoholic oxygen atom O(3) that is not so regular. One bromide anion trans to O(3) completes its coordination sphere. This bromide anion is 2.4813(9) Å from nickel, almost identical with the range given in the literature [32]. The second Br^- ion resides in the region of the OH group and the bromide is linked by a hydrogen bond to the alcoholic proton attached to the oxygen atom that is bound to the nickel center, the Br(2)···H(3) distance is 2.203 Å.

Another interesting feature is the presence of hydrogen bonding between Br(1) (coordinated bromide ion) of one molecule and H at C(2) of another molecule; the Br(1)···H distance is 2.813 Å. Therefore, the $NiLBr^+$ cations are held together in pairs by intermolecular

Table 3
Selected bond lengths (Å) bond angles (°) for **2b**·CH_3CN and **2b**·1.75CH_3CN

	2b·CH_3CN	**2b**·1.75CH_3CN
Bond lengths		
Ni(1)–N(1)	2.007(4)	2.004(4)
Ni(1)–N(2)	2.008(4)	2.008(4)
Ni(1)–O(1)	2.080(3)	2.098(3)
Ni(1)–O(2)	2.085(3)	2.096(3)
Ni(1)–O(3)	2.119(4)	2.125(3)
Ni(1)–Br(1)	2.4813(9)	2.4723(11)
Bond angles		
N(1)–Ni(1)–N(2)	99.91(15)	99.52(16)
N(1)–Ni(1)–O(1)	88.46(14)	87.51(14)
N(2)–Ni(1)–O(1)	167.47(14)	168.81(15)
N(1)–Ni(1)–O(2)	168.57(15)	168.29(14)
N(2)–Ni(1)–O(2)	88.00(14)	89.07(14)
O(1)–Ni(1)–O(2)	82.47(11)	82.84(12)
N(1)–Ni(1)–O(3)	95.18(15)	95.63(14)
N(2)–Ni(1)–O(3)	92.12(14)	92.07(14)
O(1)–Ni(1)–O(3)	77.47(12)	78.51(12)
O(2)–Ni(1)–O(3)	76.15(12)	75.98(13)
N(1)–Ni(1)–Br(1)	95.15(13)	95.39(12)
N(2)–Ni(1)–Br(1)	96.61(11)	95.14(11)
O(1)–Ni(1)–Br(1)	91.87(9)	92.82(10)
O(2)–Ni(1)–Br(1)	92.09(10)	91.72(9)
O(3)–Ni(1)–Br(1)	165.12(9)	165.65(9)

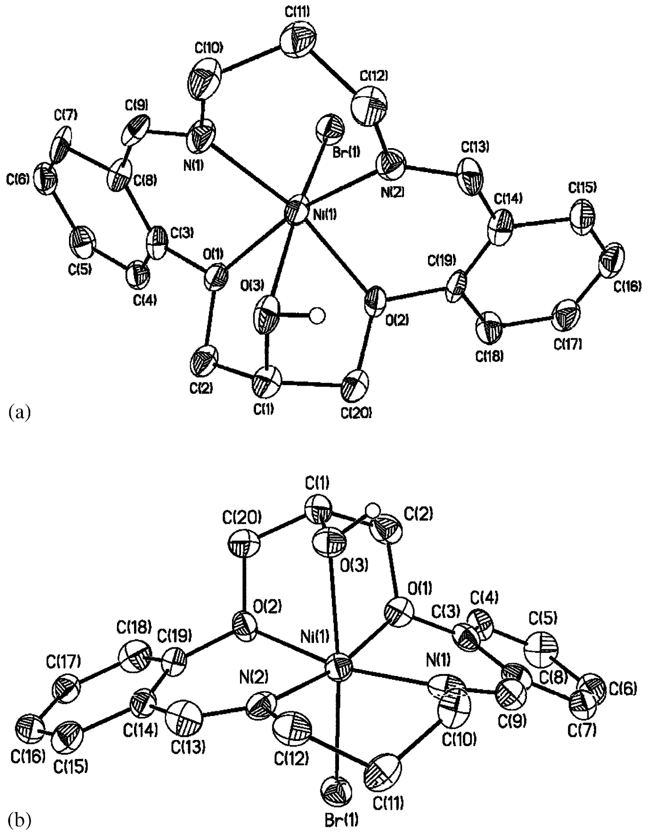

Fig. 1. ORTEP representation of the solid-state molecular structures for (a) **2b**·CH_3CN, (b) **2b**·1.75CH_3CN. Hydrogen atoms and Br^- counterions are omited for clarity.

hydrogen bonds (see Fig. 2). Apart from the different bond lengths to the nickel for donor types (O, N, Br), the most marked distortions from regular octahedral coordination are the considerable deviation from 90° that we observed for several of the angles subtended the nickel by adjacent donor atoms of the macrocycle. Two chelate rings incorporating the aromatic rings are bent to the same side. The coordination geometries on Ni(II) in **2b**·CH_3CN and **2b**·1.75CH_3CN are quite similar, only differing in the packing modes in the crystals and hydrogen bonds (see Fig. 2). In **2b**·1.75CH_3CN crystals all the $NiLBr^+$ cations are linked together by hydrogen bonds and have a network solid structures. Such a different packing pattern between the two crystals led to very slight differences of the bond lengths and angles in the two complexes.

4. Conclusion

The macrocyclic Schiff base ligand derived from 2-[3-(2-formylphenoxy)-2-hyroxypropoxy] benzaldehyde, and 1,3-diaminopropane in presence of Ni(II) salts is able to coordinate nickel(II) as five-coordinate ligand. The six-coordinate complexes possess a anion in one of the axial positions. Characterization of solutions of the obtained complexes by spectroscopic and conductivity techniques is consistent with the solid-state X-ray crystal structure of the complexes.

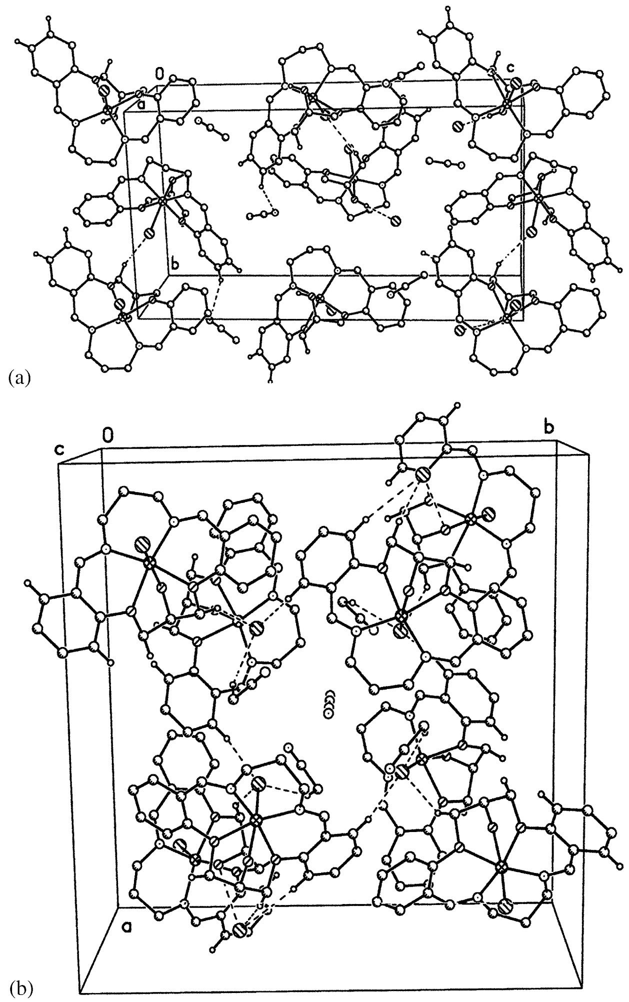

Fig. 2. Unit cell packing diagrams for (a) **2b**·CH_3CN, (b) **2b**·1.75CH_3CN.

5. Supplementary material

Crystallographic data for the structural analysis have been deposited with the Cambridge Crystallographic Data Centre, CCDC Nos. 198390 and 198389 for **2b**·CH_3CN and **2b**·1.75CH_3CN, respectively. Copies of this information may be obtained free of charge from The Director, CCDC, 12 Union Road, Cambridge, CB2 1EZ, UK (fax: +44-1223-336033; e-mail: deposit@ccdc.cam.ac.uk or www: http://www.ccdc.cam.ac.uk).

Acknowledgements

We are grateful to Tabriz University Research Council for the financial support of this research. We thank Prof. Alexander Yanovsky's group for the X-ray crystal structure determination.

References

[1] S. Kopolow, T.E. Hogen-Esch, J. Smid, Macromolecule 6 (1973) 133.

[2] L.F. Lindoy, H.C. Lip, L.F. Power, J.H. Rea, Inorg. Chem. 15 (1976) 1724.

[3] J. Lisowski, P. Starynowicz, Inorg. Chem. 38 (1999) 1351.

[4] D. Esteban, R. Bastida, A. Blas, A. Macias, A. Rodriguez, T. Rodriguez-Blas, D.E. Fenton, H. Adams, J. Mahia, Inorg. Chem. 38 (1999) 1937.

[5] A.L. Vance, N.W. Alcock, D.H. Busch, J.A. Heppert, Inorg. Chem. 36 (1997) 5132.

[6] A. Ekstrom, L.F. Lindoy, R.J. Smith, Inorg. Chem. 19 (1980) 724.

[7] A. Ekstrom, L.F. Lindoy, H.C. Lip, R.J. Smith, H.J. Goodwin, M. McPartlin, P.A. Tasker, J. Chem. Soc., Dalton Trans. (1979) 1027.

[8] G. Anderegg, A. Ekstrom, L.F. Lindoy, R.J. Smith, J. Am. Chem. Soc. 102 (1980) 2670.

[9] K.R. Adam, L.F. Lindoy, B.W. Skelton, S.V. Smith, A.H. White, J. Chem. Soc., Dalton Trans. (1994) 3361.

[10] D.E. Fenton, B.P. Murphy, A.J. Leong, L.F. Lindoy, A. Bashall, M. McPartlin, J. Chem. Soc., Dalton Trans. (1987) 2543.

[11] K.R. Adam, L.F. Lindoy, H.C. Lip, J.H. Rea, B.W. Skelton, A.H. White, J. Chem. Soc., Dalton Trans. (1981) 74.

[12] K. Henrick, L.F. Lindoy, M. McPartlin, P.A. Tasker, M.P. Wood, J. Am. Chem. Soc. 106 (1984) 1641.

[13] L.A. Drummond, K. Henrick, M.J.L. Kanagasundaram, L.F. Lindoy, M. McPartlin, P.A. Tasker, Inorg. Chem. 21 (1982) 3923.

[14] A. Berkessel, M. Bolte, T. Newmann, L. Seidel, Chem. Ber. 129 (1996) 1183.

[15] J.R. Lancaster (Ed.), The Bioinorganic Chemistry of Nickel, VCH, New York, 1988.

[16] A.F. Kolodziej, Prog. Inorg. Chem. 41 (1994) 493.

[17] V. Dudler, L.F. Lindoy, D. Sallin, C.W. Schlaepfer, Aust. J. Chem. 40 (1987) 1557.

[18] J.H. Camero, H.B. Harvey, I. Soutar, J. Chem. Soc., Dalton Trans. (1992) 597.

[19] B.S. Furniss, A.J. Hannaford, P.W.G. Smith, A.R. Tachell (Eds.), Vogel's Textbook of Practical Organic Chemistry, 5th ed., Longman, London, 1989.

[20] D.D. Perrin, W.L.F. Armarego (Eds.), Purification of Laboratory Chemicals, 3rd ed., Pergamon Press, Oxford, 1988.

[21] G. Brauer (Ed.), Handbook of Preparative Inorganic Chemistry, 2nd ed., Academic Press, New York, 1963.

[22] G. Braun, Org. Synth. II (1943) 308.

[23] L.F. Lindoy, L.G. Armstrong, Inorg. Chem. 14 (1975) 1322.

[24] Bruker SMART, Version 5.059, Bruker Molecular Analysis Research Tool, Bruker AXS, Madison, WI, 1998.

[25] Bruker SAINT-PLUS, Version 6.01, Data Reduction and Correction Program, Bruker AXS, Madison, WI, 1998.

[26] G.M. Sheldrick, SADABS, Version 2.01, Bruker/Siemens Area Detector Absorption Correction Program, Bruker AXS, Madison, WI, 1998.

[27] G.M. Sheldrick, SHELXTL, Version 5.10, Structure Determination Software Suite, Bruker AXS, Madison, WI, 1998.

[28] International Tables for Crystallography, Tables 4.2.6.8 and 6.1.1.4, vol. C, Kluwer Academic Publishers, Dordrecht, Netherlands, 1992.

[29] K.R. Adam, G. Anderegg, L.F. Lindoy, H.C. Lip, M. McPartlin, J.H. Rea, R.J. Smith, P.A. Tasker, Inorg. Chem. 19 (1980) 2956.

[30] W.J. Geary, Coord. Chem. Rev. 7 (1971) 81.

[31] A.B.P. Lever, Inorganic Electronic Spectroscopy, 2nd ed, Elsevier, Amsterdam, 1984.

[32] H.J. Goodwin, K. Henrick, L.F. Lindoy, M. McPartlin, P.A. Tasker, Inorg. Chem. 21 (1982) 3261.